Development of a Control Algorithm for Active Control of Rolling Motion of a Ship by Gyro-Stabilizer

Ki-Seok Song[1], Soo-Min Kim[1], Moon K. Kwak[1], Weidong Zhu[2]

[1]Department of Mechanical, Robotics and Energy Engineering,

Dongguk University-Seoul, 30 Pildong-ro 1gil, Jung-gu, Seoul 04620, Korea

[2]Department of Mechanical Engineering,

University of Baltimore of Maryland County, 1000 Hilltop Circle, Baltimore, MD 21250

Total number of pages = 33

Number of Figures = 9

Number of Tables = 0

Number of Appendices = 0

Corresponding author:

Prof. Moon K. Kwak

Department of Mechanical, Robotics and Energy Engineering

Dongguk University-Seoul

Pildong-ro 1gil 30, Jung-gu,

Seoul 04620, KOREA

Fax : +82-2-2263-9379

Phone: +82-2-2260-3705

E-mail: kwakm@dongguk.edu

Abstract

In this study, a new algorithm for an active gyro-stabilizer was developed and applied to a ship model. The active gyro-stabilizer consists of a gyro sensor that measures the angular velocity of the rolling motion of a ship, a controller that realizes the active control algorithm, and an actuator that is connected to the precession axis. The new control algorithm receives the rolling rate of the ship, and outputs the desired precession angle. A suitable actuator for this kind of mission could be a servomotor. First, a theoretical model with a passive gyro-stabilizer was investigated to show the working mechanism of the gyro-stabilizer. It was found that the passive gyro-stabilizer works as additional stiffness. Based on the equations of motion of the ship with a gyro-stabilizer, a new control strategy for an active gyro-stabilizer was developed. It was found theoretically that instead of increasing stiffness, the damping of the rolling motion of the ship could be increased by tuning the filter frequency of the control algorithm to the rolling frequency. Both numerical and experimental results showed that the proposed control algorithm is valid and cost-effective, because it does not require a high-speed and heavy spinning wheel.

Keywords: Gyro-stabilizer, Active control algorithm, active roll damping.

1. Introduction

Because ships run on water, they are constantly moved by waves or wind. The movement of a ship consists of six degrees of freedom, which are three types of translational motion: surge, sway, and heave, and three types of rotational motion: roll, pitch, and yaw. Among them, the rotational motion about the surge axis is called rolling, and the rolling motion can lead to problems such as seasickness and the safety of sailors, as well as ship rollover accidents. For this reason, efforts have been made to prevent or reduce rolling by installing additional devices on ships.

Typical roll reduction devices used to control rolling include the bilge keel, anti-rolling tank, fin stabilizer, and gyro-stabilizer (Perez, 2005). The bilge keel is in the form of a thin plate like a fin, and is installed on both sides at the lower end of the ship. As the hull is tilted, the hydrodynamic resistance is increased by the bilge keel (Lewis, 1989). However, rolling cannot be effectively controlled with only the bilge keel.

An anti-rolling tank is a kind of large tank installed inside the ship, and filled with water. The anti-rolling tank can be thought of as a tuned mass damper for the rolling motion, using sloshing as a dynamic absorber. Depending on the shape of the tank, it is divided into a free surface tank, a U-tube tank, and an external tank; and of these, the most commonly used type is the U-tube tank. This device is again divided into passive and active types depending on its working mechanism. The passive type allows the fluid inside the tank to move freely when the ship makes a rolling motion, and the sloshing frequency is tuned to the rolling frequency. Although the passive device shows good performance in the ship's rolling frequency band, the

amplitude increases in the low-frequency region, resulting in poor stability (Perez, 2005). To improve stability in the low-frequency region, instead of a passive type, an active type is mainly used that artificially manipulates the flow rate and phase difference inside the tank by installing a pump or valve in the middle. However, since the anti-rolling tank must be installed inside the ship, there is the disadvantage that the internal space of the ship must be used. In addition, as a large control force is required, the size of the tank should be increased, but because of internal space limitations, that may not be possible.

There are two main types of stabilizers to control rolling: the fin, and the gyro. The fin stabilizer is a device that controls rolling using lift and descent forces generated by properly rotating fins, which are fin-like structures that are attached to both sides of a submerged hull. This is used as a basic active rolling reduction device as a system for rotating fins by detecting the degree of inclination of the hull. However, the structure of fin stabilizers is complicated, so installation costs are expensive, and maintenance is difficult. In addition, there is a disadvantage, in that while the ship is anchored, lift and descent forces are not generated, so rolling can be controlled only during cruising. Recently, a fin stabilizer using a curved fin instead of a flat one has been developed, which makes rolling control possible even when the ship is anchored (Perez and Blanke, 2012). However, compared with the gyro-stabilizer, the control effect at the time of anchoring is insignificant.

The gyro-stabilizer is a device that suppresses the roll of a structure using a torque generated using the principle of the gyroscope. When the hull is rolled by waves or wind, the device controls the roll through precession, which generates a torque in the opposite direction.

Although the gyro-stabilizer is installed in the hull, it offers higher space utilization than other devices and is easy to maintain. In addition, there is the advantage that the rolling may be effectively controlled even during anchoring. This study is concerned with the active gyro-stabilizer that may exhibit excellent performance regardless of operating conditions.

Research to control the rolling of ships using gyro-stabilizers was investigated during the late 19th and early 20th centuries. In 1904, Schlick first attempted to install a gyro-stabilizer on a ship to control its rolling (Schlick, 1904a, 1904b). The initial gyro-stabilizer was a passive type device, which had problems adjusting the precession moment according to the magnitude of the waves. The gyro-stabilizer worked well on the vessel Schlick used, but it did not perform as expected in other vessels (Chalmers, 1931). In 1915, Sperry developed an active gyro-stabilizer that overcame the shortcomings of Schlick's gyro-stabilizer (Sperry, 1915; Perez, 2005). The active gyro-stabilizer at this time made the precession angular velocity proportional to the roll rate. Sperry's gyro-stabilizer was actually used for warships and ferries with excellent rolling reduction effect. But the gyro-stabilizer was shunned because of problems such as weight and cost, and the advent of the fin stabilizer. After that, in the 1990s, thanks to the development of motors, materials, and control engineering, gyro-stabilizers, which exhibit excellent rolling control capabilities even when the ship is anchored, began to once again attract attention. Jones (1967) described the fact that the anti-resonant frequency of a gyroscopic vibration absorber (GVA) is a linear function that is proportional to the rotational speed of the rotor, so that the GVA can be easily synchronized and applied to vehicles and machinery having variable frequency vibration excitation, and the analytical results were demonstrated through experiments. Perez and Steinmann (2009) designed a proportional-derivative

controller, assuming that the control torque of the precession angle appears as a linear combination of the precession angle and the precession angular velocity, using the dynamic model of the structure equipped with the active gyro-stabilizer. In addition, theoretical simulation was conducted using a JONSWAP wave spectrum for the system including the designed controller. Townsend and Shenoi (2014) introduced a dynamic model for twin-type gyro-stabilizer systems with a vertical precession axis, and presented four control methods: passive control, derivative-based control, reaction wheel control, and unrestricted gimbal control. Furthermore, theoretical simulation using the JONSWAP wave spectrum was performed for each control method. Poh et al. (2017) used a dynamic model like Perez and Steinmann (2009), but designed the proportional-integral controller so that the precession torque is the linear combination of the roll angle and the integral term of the roll angle of the hull. In addition, several companies, like SeaKeeper in the United States and Mitsubishi Heavy Industries (MHI) in Japan have developed active gyro-stabilizers and applied them to yachts of different sizes. SeaKeeper's gyro-stabilizer minimizes friction and heat generation by allowing the rotor to rotate at high speed in a vacuum environment, and eliminates the roll from (70 to 98) % depending on several conditions (Seakeeper, 2022). In the case of MHI, anti-rolling gyro(ARG) had a 70 % roll reduction at zero speed (Takeuchi et al., 2011).

The gyro-stabilizer has also been applied to various structures. Ünker and Çuvalcı (2015) used a passive gyro-stabilizer to stabilize an inverted pendulum-type structure. The Lagrange equation was used to obtain the equations of motion, and the numerical calculations were performed to calculate the response of the system according to the rotational speed of the rotor. Furthermore, an experiment was conducted to demonstrate the validity of the induced system

through comparison with the results of numerical calculations (Ünker and Çuvalcı, 2016). Manmathakrishnan and Pannerselvam (2021) added a gyro-stabilizer to a barge equipped with an offshore wind turbine, and conducted dynamic modeling. After that, the experiments were conducted using a 1:50 scale model under three conditions with different rotational speeds of the turbine rotor.

In this study, a simple dynamic model with gyro-stabilizers was first introduced to develop a control algorithm for the active gyro-stabilizer. Based on the coupled equations of motion, the characteristics and expected effects of the passive gyro-stabilizers were described. Then, a new control algorithm for the active gyro-stabilizer based on the servomotor mechanism was developed. To verify the validity of the new control algorithm, experiments were conducted using a small-scale ship model manufactured with a 3D printer. The ship model is a semi-circular cylindrical shell equipped with the active gyro-stabilizer consisting of a rotor connected to a BLDC motor, a MEMS-type gyro sensor, and an RC servomotor that can control the precession angle. Experimental results show the effectiveness of the proposed control algorithm.

2. Dynamic model of a ship equipped with a passive gyro-stabilizer

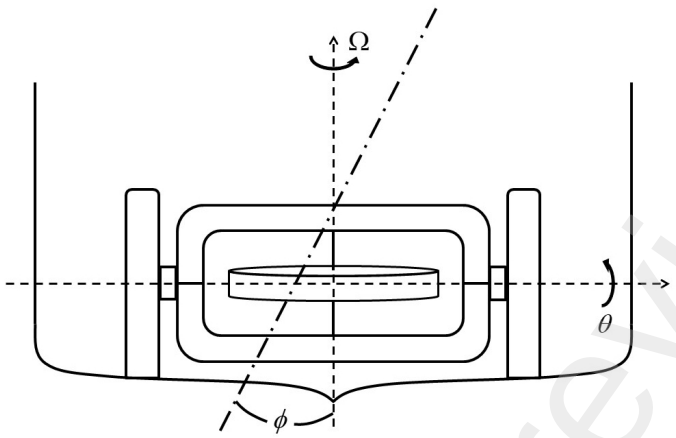

Fig. 1. Dynamic model of a ship equipped with a gyro-stabilizer.

Fig. 1 shows a ship model equipped with a passive gyro-stabilizer. In Fig. 1, θ, ϕ, and Ω represent the precession angle of the gyro-stabilizer, the rolling angle of the hull, and the rotational speed of the rotor, respectively. The roll and precession angles are assumed to be small, and the precession axis of the gyro-stabilizer is fixed to the axis of the pitch axis, which is orthogonal to the roll axis (Townsend et al., 2007). Then, the well-known equations of motion that describe the coupled rolling motion of the ship and the precession motion of the gyro can be derived using the Lagrange equation with the kinetic and potential energy of the system (Harris and Piersol, 2002):

$$I_s\ddot{\phi} + c_s\dot{\phi} + k_s\phi + I\Omega\dot{\theta} = m_w \tag{1}$$

$$I_g\ddot{\theta} + c_g\dot{\theta} + k_g\theta - I\Omega\dot{\phi} = 0 \tag{2}$$

where I_s is the mass moment of inertia of the ship, c_s is the damping coefficient of the ship,

k_s is the stiffness coefficient of the ship, I_g is the mass moment of inertia of the gyro-stabilizer that is associated with the simple pendulum motion, c_g is the damping coefficient of the newly added gyro-stabilizer, k_g is the stiffness coefficient of the gyro-stabilizer, I is the mass moment of inertia of the gyro-stabilizer rotor, and m_w is the external disturbance moment by the waves. Dividing Eq. (1) by I_s and Eq. (2) by I_g yields the following equations of motion:

$$\ddot{\phi} + 2\zeta_s \omega_s \dot{\phi} + \beta \omega_s \dot{\theta} + \omega_s^2 \phi = \omega_s^2 \bar{m}_w \tag{3}$$

$$\ddot{\theta} - \frac{\beta \omega_s}{\alpha} \dot{\phi} + 2\zeta_g \omega_g \dot{\theta} + \omega_g^2 \theta = 0 \tag{4}$$

where,

$$\omega_s = \sqrt{\frac{k_s}{I_s}}, \quad \omega_g = \sqrt{\frac{k_g}{I_g}}, \quad \zeta_s = \frac{c_s}{2I_s\omega_s}, \quad \zeta_g = \frac{c_g}{2I_g\omega_g} \tag{5a-d}$$

$$\beta = \frac{I\Omega}{I_s\omega_s}, \quad \alpha = \frac{I_g}{I_s}, \quad \bar{m}_w = \frac{m_w}{I_s\omega_s^2} \tag{5e-g}$$

in which, ω_s is the rolling natural frequency of the ship, ω_g is the precession natural frequency of the gyro, ζ_s and ζ_g are the damping ratios of the rolling motion of the ship and the precession of the gyro, respectively, β is the ratio of the angular momentum of the rotor of the gyro to the angular momentum of the ship, α is the ratio of the mass moment of inertia of the ship to the gyro, and $\bar{m}_w$ is the nondimensionalized external excitation moment

of the waves.

If a gyro-stabilizer is not installed, then only the ship motion equation remains and can be reduced to:

$$\ddot{\phi} + 2\zeta_s \omega_s \dot{\phi} + \omega_s^2 \phi = \omega_s^2 \bar{m}_w \tag{6}$$

Hence, the transfer function of the ship roll motion without the gyro becomes:

$$\frac{\bar{\Phi}(s)}{\bar{M}_w(s)} = G_u(s) = \frac{\omega_s^2}{s^2 + 2\zeta_s \omega_s s + \omega_s^2} \tag{7}$$

Inserting $s = j\omega_s$ into Eq. (7), the peak amplification ratio of the roll motion of the ship without gyro can be written as:

$$P_u = \left| G_u(j\omega_s) \right| = \frac{1}{2\zeta_s} \tag{8}$$

where, $j = \sqrt{-1}$.

The easiest way to use a passive gyro-stabilizer is to place the gyro's center of gravity on the axis of precession, so that $\omega_g \simeq 0$, and to make the viscous damping of the precession as small as possible, thus making $\zeta_g \simeq 0$. In this way, the simplified relation between the roll rate and the precession angle can be derived from Eq. (4):

$$\dot{\theta} = \frac{\beta \omega_s}{\alpha} \phi \tag{9}$$

Substituting Eq. (9) into Eq. (3) yields the simplified equation of motion for the rolling of the

ship with the passive gyro, which can be derived as follows:

$$\ddot{\phi} + 2\zeta_s \omega_s \dot{\phi} + \omega_s^2 \left(1 + \frac{\beta^2}{\alpha}\right)\phi = \omega_s^2 \bar{m}_w \tag{10}$$

Hence, the approximate transfer function of the ship roll motion with the passive gyro becomes:

$$\frac{\bar{\Phi}(s)}{\bar{M}_w(s)} = G_{pa}(s) = \frac{\omega_s^2}{s^2 + 2\zeta_{sn}\omega_{sn}s + \omega_{sn}^2} \tag{11}$$

where,

$$\omega_{sn} = \omega_s \sqrt{1 + \frac{\beta^2}{\alpha}}, \qquad \zeta_{sn} = \zeta_s \frac{\omega_s}{\omega_{sn}} = \zeta_s \Big/ \sqrt{1 + \frac{\beta^2}{\alpha}} \tag{12}$$

What is immediately apparent from Eq. (10) is that a well-designed passive gyro-stabilizer can increase the roll stiffness of the ship against wave excitation. Once the size of the rotor of the gyro is determined and the structure to support the gyro is designed, I and I_g are determined. It is desirable to make I_g as small, and I as large, as possible. However, due to the structural limitations of the ship and the gyro, it is not easy to make the values of I_g and I as are wanted. Rather, the greater the angular velocity Ω of the rotor of the gyro, the more advantageous it is. That is, by increasing the performance of the motor connected to the axis of the rotor and rotating at high speed, the rolling motion can be reduced by the mass moment of inertia of the small rotor. This means that it is possible to make the rolling stiffness large, so that it may counteract the external excitation moment. However, an expensive motor must be used to make the high-speed rotation, and there are many things to consider, such as balancing

the gyro rotor, and minimizing the wear of gyro bearings due to the high-speed rotation. As the rolling stiffness of the ship increases, naturally the rolling response of the ship to the external excitation moment decreases. However, as the rolling natural frequency increases, the ship may experience a high-frequency rolling.

The peak amplification ratio of the roll motion of the ship with passive gyro can be written as follows by inserting $s = j\omega_{sn}$ into Eq. (11):

$$P_{pa} = \left|G_{pa}(j\omega_{sn})\right| = \frac{1}{2\zeta_s\sqrt{1+\frac{\beta^2}{\alpha}}} \tag{13}$$

It is evident from Eqs. (12) and (13) that the introduction of the passive gyro increases the rolling stiffness, resulting in high natural frequency and low damping, but the peak amplitude of the ship with the passive gyro is still less than the peak amplitude of the ship without the passive gyro.

Using the fully coupled equations of motion given by Eqs. (3) and (4), the block diagram of the system with the passive gyro can be drawn as Fig. 2:

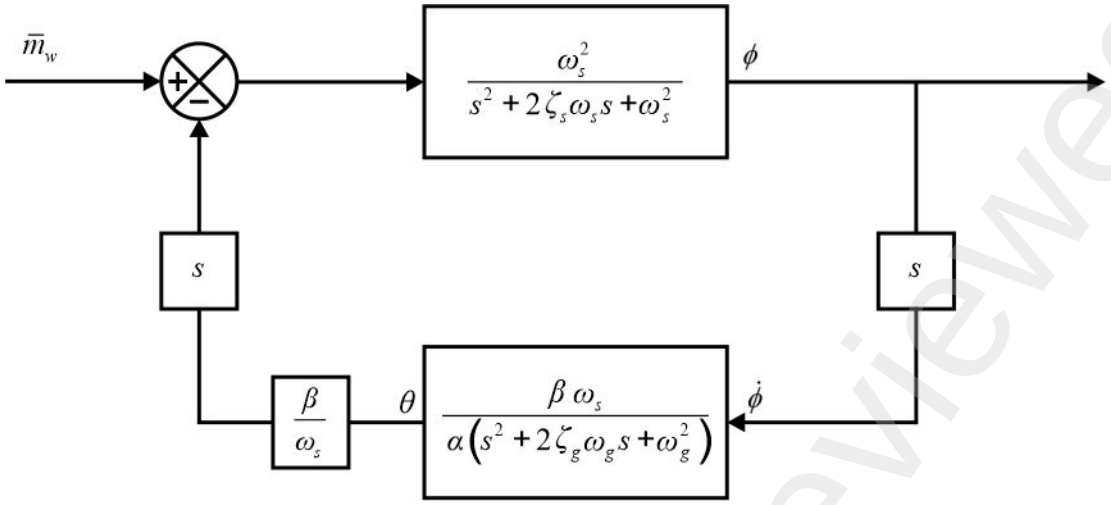

Fig. 2. Closed-loop block diagram of the ship with the passive gyro-stabilizer.

The closed-loop transfer function can be derived based on the block diagram given in Fig. 2:

$$\frac{\bar{\Phi}(s)}{\bar{M}_w(s)} = G_p(s) = \frac{N_p(s)}{D_p(s)} \tag{14}$$

where,

$$N_p(s) = (s^2 + 2\zeta_g\omega_g s + \omega_g^2)\omega_s^2 \tag{15a}$$

$$\begin{aligned} D_p(s) = s^4 + 2\left(\zeta_s\omega_s + \zeta_g\omega_g\right)s^3 + \left(\omega_s^2 + \omega_g^2 + 4\zeta_s\zeta_g\omega_s\omega_g + \frac{\beta^2\omega_s^2}{\alpha}\right)s^2 \\ + 2\omega_s\omega_g\left(\zeta_g\omega_s + \zeta_s\omega_g\right)s + \omega_s^2\omega_g^2 \end{aligned} \tag{15b}$$

Naturally, if we set $\omega_g = \zeta_g = 0$, then $G_p(s)$ reduces to $G_{pa}(s)$ of Eq. (11). The closed-loop system given by Eq. (14) is stable by the Routh-Hurwitz criteria.

To confirm the conclusions based on the theoretical model, numerical calculations were

carried out using the fully-coupled equations of motion, Eqs. (7) and (14). To this end, the following parameter values were used:

$$\omega_g / \omega_s = 0.0001,\ \ \zeta_s = 0.05,\ \ \zeta_g = 0.0001,\ \ \alpha = 0.01,\ \ \beta = 0.2$$

Fig. 3 shows the theoretical Bode plots of the ship model without the gyro-stabilizer (dotted line), and equipped with the passive gyro-stabilizer (solid line). As expected by the theoretical study, and shown in Fig. 3, the rolling stiffness of the ship equipped with the passive gyro-stabilizer increases, and the natural roll frequency is shifted to the right, which implies a higher natural roll frequency. Of course, as β increases, the roll frequency increases. Passengers on board may experience high-frequency vibrations because of this problem. However, it can be found from Fig. 3 that with the introduction of the passive gyro-stabilizer, the peak amplitude decreases. In general, the response to external excitation moment driven by water waves in the low-frequency band can be significantly suppressed. But for a passive gyro-stabilizer to be effective, either the mass moment of inertia of the rotor must be large or the angular velocity of the rotor must be fast enough to obtain a high value of β.

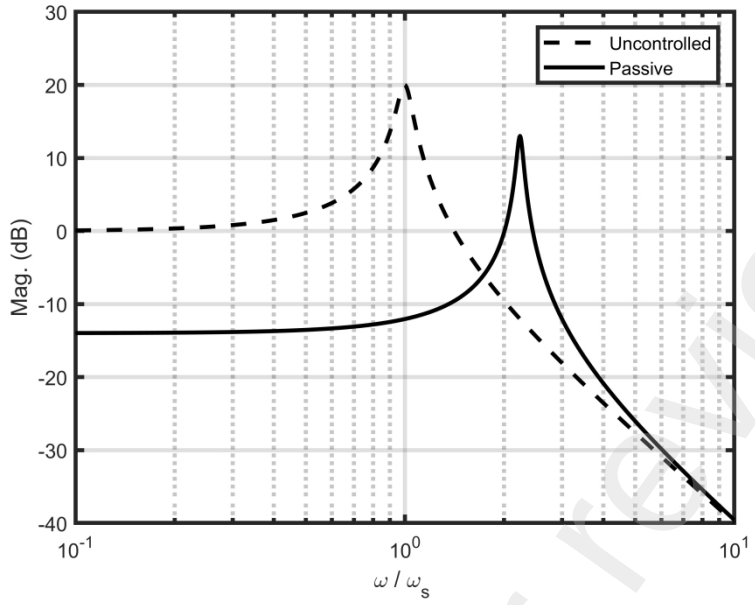

(a) Magnitude

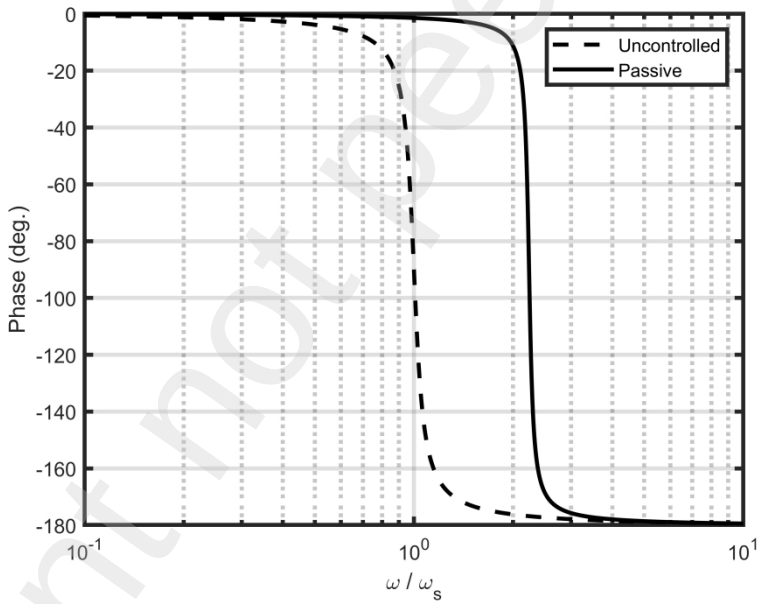

(b) Phase

Fig. 3. Theoretical Bode plots of roll angle w/ and w/o the passive gyro-stabilizer.

3. Dynamic model of a ship equipped with an active gyro-stabilizer

When an external excitation moment causes a structure to roll, the passive gyro-stabilizer attached to the structure starts precession, and generates torque in the opposite direction to counteract the external moment, which acts by itself corresponding to the external moment. To this end, it is desired to increase the rolling stiffness so that $\omega_g \simeq 0$ and $\zeta_g \simeq 0$. On the other hand, an active gyro-stabilizer is a device that, when rolling occurs in a ship, measures the rolling rate using a sensor, and controls the precession according to the control algorithm. To control the precession movement, an appropriate actuator must be connected to the precession axis. In the study of the active gyro-stabilizer (Perez and Steinmann, 2009), it was assumed that the motor axis is directly connected to the precession axis and additional control moment is applied to the precession axis, which amounts to adding the control moment term to the right-hand side of Eq. (4). However, considering the fact that almost all motors use gears to amplify the torque, there is no real actuator that can generate sufficient moment in this way by connecting the motor directly to the precession axis without gears. Also, the control design becomes complicated.

In this study, the use of a geared servomotor is considered for real applications. The servomotor is capable of tracing the angle of the driving axis very accurately by the internal PID control algorithm. Hence in this study, a new control algorithm that can produce the desired precession angle is developed. In fact, the new control algorithm is also based on the equation of motion of the passive gyro-stabilizer, Eq. (4). The proposed control algorithm is as follows:

$$\frac{\bar{\Theta}_c(s)}{\bar{\dot{\Phi}}(s)} = \frac{g\beta\omega_s}{\alpha\left(s^2 + 2\zeta_g\omega_s s + \omega_s^2\right)} \tag{16}$$

where $\bar{\Theta}_c(s)$ and $\bar{\dot{\Phi}}(s)$ are the Laplace transforms of $\theta_c(t)$ and $\dot{\phi}(t)$, and g is the control gain. A subscript c is added to the precession angle to differentiate it from the passive system. The new control algorithm uses the roll rate instead of the roll angle, which is very practical, because a gyro sensor normally measures angular velocities. The sensors usually used to measure angular motion are gyro sensors, which require the use of techniques such as Kalman-Filtering and Offset-Removal to estimate the actual rolling angle of the ship. However, over time, it is difficult to estimate the exact rolling angle, due to the influence of drift. This is why we adopt the roll rate, instead of the roll angle. The proposed new active control algorithm uses the roll rate directly, so that it is very simple to use for real applications.

Because the output of the control algorithm is the desired precession angle, the desired precession angle is to be traced by the servomotor controller using the internal PID control algorithm. The new algorithm is mainly based on the theory of the tuned mass damper, so that we tune the natural frequency of the controller to the ship's natural frequency, which means $\omega_g = \omega_s$. In this case, an active damping effect can be obtained at resonance, and thus the resonance amplitude is greatly suppressed. Because we need a broader frequency bandwidth to cope with the wide frequency bands of water waves, $\zeta_g = 0.3$ is proposed, as in the case of the positive position feedback control (Fanson and Caughey, 1990), and the negative acceleration feedback control algorithm for the active tuned mass damper (Yang et al., 2017). The proposed new active control algorithm increases the roll damping of the ship, not the

rolling stiffness. The new control algorithm given by Eq. (16) is referred to as an angular rate feedback control (ARFC). Combining Eq. (7) and Eq. (16), a closed-loop control system is expressed as shown in Fig. 4:

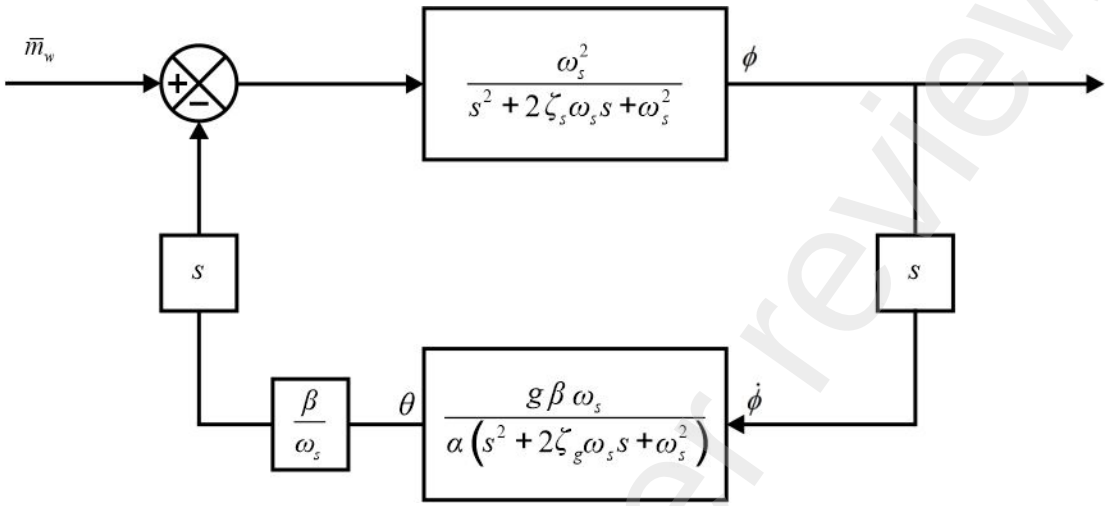

Fig. 4. Closed-loop block diagram of the ship with the active gyro-stabilizer.

The transfer function of the closed-loop system with the active gyro algorithm can be written as follows:

$$\frac{\bar{\Phi}(s)}{\bar{M}(s)} = G_c(s) = \frac{N_c(s)}{D_c(s)} \tag{17}$$

where,

$$N_c(s) = (s^2 + 2\zeta_g\omega_s s + \omega_s^2)\omega_s^2 \tag{18a}$$

$$\begin{aligned} D_c(s) = {} & s^4 + 2\left(\zeta_g + \zeta_s\right)\omega_s s^3 + \left(2 + 4\zeta_g\zeta_s + \frac{\beta^2}{\alpha}g\right)\omega_s^2 s^2 \\ & + 2\left(\zeta_g + \zeta_s\right)\omega_s^3 s + \omega_s^4 \end{aligned} \tag{18b}$$

Applying the Routh-Hurwitz criteria to Eq. (18b), it can be seen that if $g > -\frac{4\alpha}{\beta^2}\zeta_s\zeta_g$, the system is unconditionally stable. That is, the proposed control algorithm has a static stable condition, and does not depend on the frequency. In this study, we simply used the positive gain.

The peak amplification ratio at the resonance can be obtained by substituting $s = j\omega_s$ in Eq. (17), as follows:

$$P_c = \left|G_c(j\omega_s)\right| = \frac{1}{2\zeta_s\left(1+\frac{g\beta^2}{4\alpha\zeta_s\zeta_g}\right)} \tag{19}$$

It can be readily understood by comparing Eq. (19) with Eqs. (8) and (13) that roll damping is actively increased. The damping factor of the closed-loop system with ARFC can be written as follows:

$$\zeta_c = \zeta_s + \frac{g\beta^2}{4\alpha\zeta_g} \tag{20}$$

Eq. (20) shows that when the active gyro-stabilizer driven by the ARFC proposed in this study is installed, the square term of β is added to the roll damping ratio of the ship. Therefore, as the angular momentum of the rotor increases, the damping force of the structure increases. In addition, the square term of β is multiplied by the control gain g, so that the damping force of the structure can be amplified without increasing the angular momentum of the rotor. The proposed control system can achieve active damping with a smaller and slower rotor than the

passive gyro, which enables a cost-effective active gyro-stabilizer to be built.

Numerical simulations were carried out with the following parameter values:

$$\omega_g / \omega_s = 1,\ \zeta_s = 0.05,\ \zeta_g = 0.3,\ \alpha = 0.01,\ \beta = 0.02,\ g = 5$$

Note here that the value of β used for the active system is one-tenth of the value used in the passive system, which implies smaller angular momentum. With these values, the total roll damping ratio can be expected to be about 0.22. Fig. 5 shows the Bode plots of the ship equipped with the active gyro-stabilizer. In Fig. 5, the dotted line represents the model without the gyro-stabilizer, while the solid line represents the model equipped with the active gyro-stabilizer. Fig. 5 shows that unlike the passive type, the damping factor surely increases, thus significantly suppressing the resonant amplitude. In addition, since the natural frequency does not increase as in the case of the passive gyro-stabilizer, high-frequency instability does not appear.

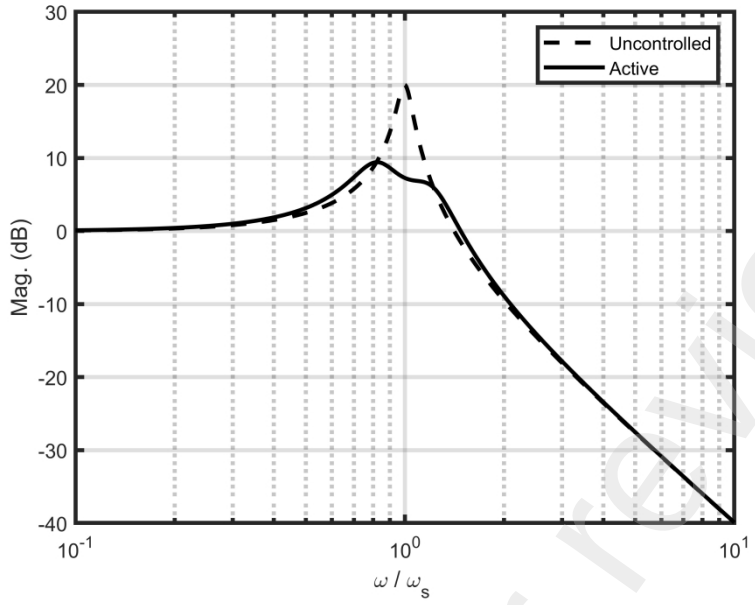

(a) Magnitude

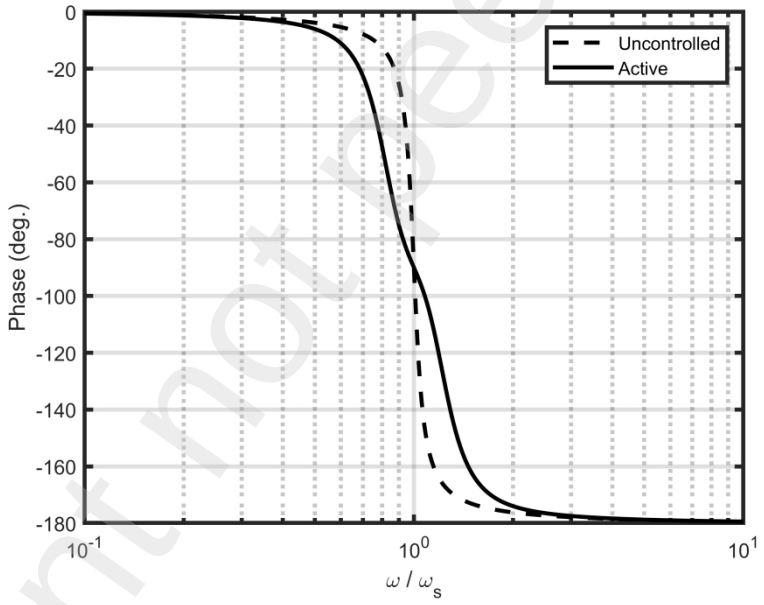

(b) Phase

Fig. 5. Theoretical frequency response curve of the roll angle.

5. Experiments

To confirm the actual operation of the theoretically verified active gyro-stabilizer, and to confirm the validity of the ARFC algorithm, a ship model was constructed, and an active control system was mounted on the model, as shown in Fig. 6. The shape of the model is a smooth cylindrical shape, so that rolling could occur easily. Fig. 6 shows the internal configuration of the experimental device:

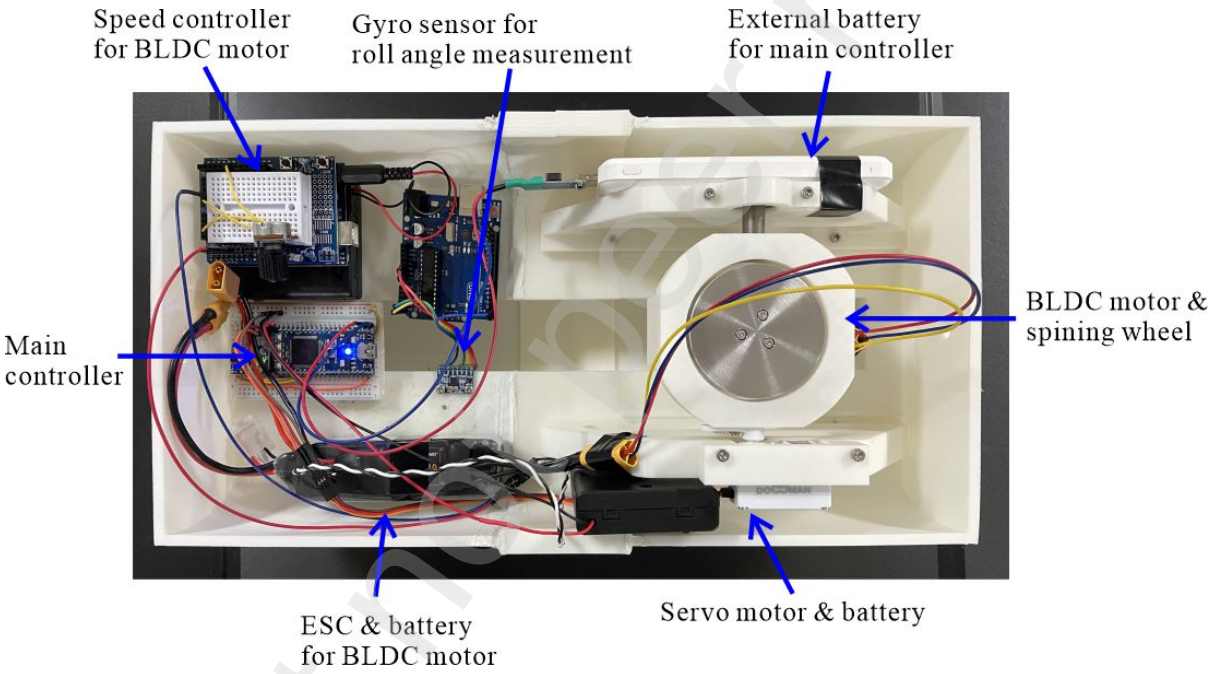

Fig. 6. Components of the experimental device.

SUNNY SKY's X2814 900KV BLDC motor was used for the motor connected to the rotor in the experimental device. Arduino Uno was used as a controller to control the rotational speed

of this BLDC motor. In addition, a gyro sensor (MPU-6050) was used to measure the roll rate of the ship model, while an RC servomotor (DM-CLS119TD) was used to accurately trace a given precession angle. The ARFC algorithm was implemented using the microcontroller (mbed NXP LPC 1768). In addition, an additional gyro sensor and controller for measuring the roll angle of the ship model, an electronic speed controller for speed and direction control of the rotor, and a lithium polymer battery and dry cell batteries were used to drive the motors and the controllers. Because the microcontroller is a digital controller, the analog form of the ARFC algorithm needs to be converted into digital form. The following bilinear transform was used to make it suitable for digital control (Tustin, 1947):

$$s = \frac{2}{T_s}\frac{z-1}{z+1} \tag{21}$$

where, T_s is the sampling period. Substituting Eq. (21) into Eq. (16), the transfer function in the digital form can be obtained as follows:

$$H_d(z) = G\frac{b_2 z^2 + b_1 z + b_0}{z^2 + a_1 z + a_0} \tag{22}$$

where, $G = g\beta / \alpha\omega_s$, and,

$$b_2 = b_0 = \frac{\omega_s^2}{\Delta}, \quad b_1 = \frac{2\omega_s^2}{\Delta} \tag{23a,b}$$

$$a_1 = \frac{2\omega_s^2 - \frac{8}{T_s^2}}{\Delta}, \quad a_0 = \frac{\frac{4}{T_s^2} - \frac{4\zeta_g\omega_s}{T_s} + \omega_s^2}{\Delta} \tag{23c,d}$$

$$\Delta = \frac{4}{T_s^2} + \frac{4\zeta_g \omega_s}{T_s} + \omega_s^2 \tag{23e}$$

Expressing Eq. (22) in the form of a discrete difference equation is necessary for C programming. The following equation that computes the desired precession angle was implemented by using C language

$$\theta_k = -a_1\theta_{k-1} - a_0\theta_{k-2} + G\left(b_2\dot{\phi}_k + b_1\dot{\phi}_{k-1} + b_0\dot{\phi}_{k-2}\right) \tag{24}$$

In the experiment, the angular velocity ($\dot{\phi}$) in the roll direction of the ship model was measured using a gyro sensor. In addition, the desired precession angle calculated using Eq. (24) was provided to the RC servomotor. A timer interrupt is required to accurately match the sampling time, and a function including a control algorithm is executed at every sampling time set using mbed's Ticker command. Within the function, the calculation was performed using the sensor value, and each variable was updated. The sampling time was set to 1 ms. The experiments were conducted in two different conditions. The first experiment was conducted on flat ground. It was carried out with the following parameter values:

$$\omega_g = \omega_s = 0.7342 \times 2\pi\,,\ \ \zeta_s = 0.03\,,\ \ \zeta_g = 0.3\,,\ \ G = 0.6$$

The values of ω_s and ζ_s were measured by the response of the free vibration without control. The total gain, *G*, was chosen based on model tests. Fig. 7 shows the results of the free-rolling experiment, and reveals that when controlled using the active gyro-stabilizer with ARFC, the rolling was rapidly suppressed.

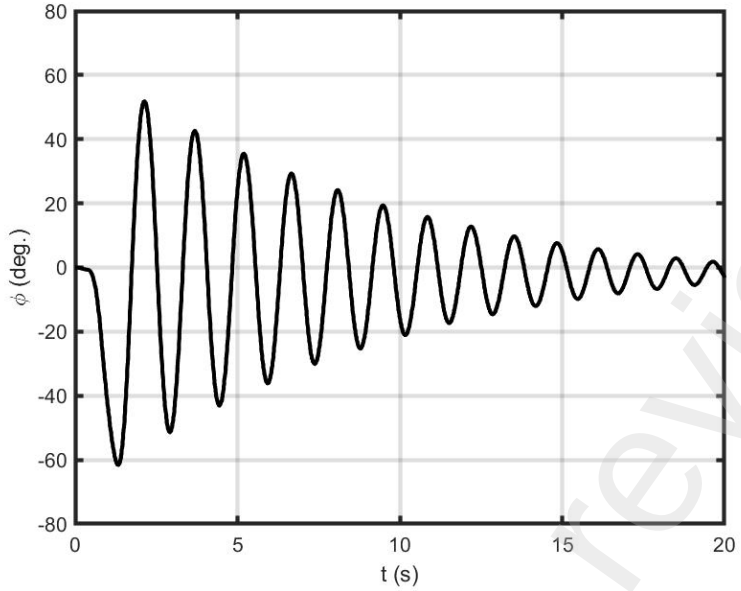

(a) Uncontrolled

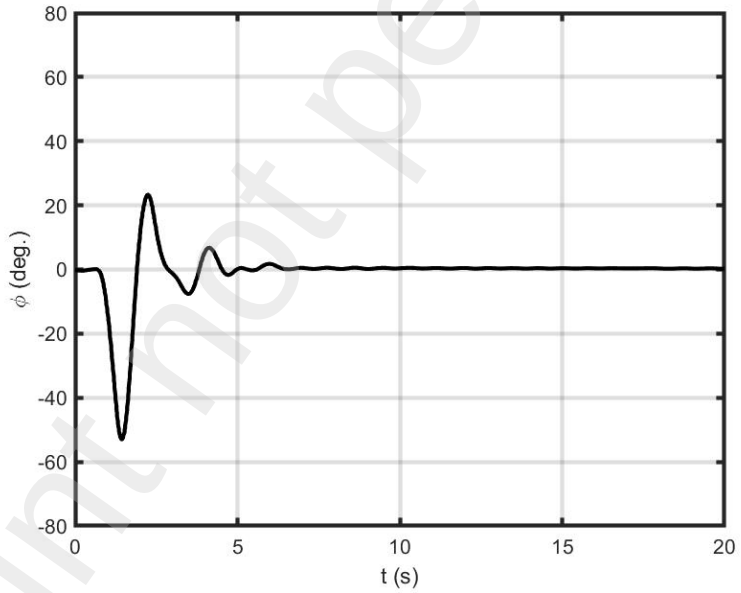

(b) Controlled

Fig. 7. Time response of the roll angle of the ship model on flat ground.

The second experiment was conducted in an acrylic tank, as shown in Fig. 8. The experiment was carried out with the following parameter values:

$$\omega_g = \omega_s = 1.0596 \times 2\pi\,,\ \ \zeta_s = 0.02\,,\ \ \zeta_g = 0.3\,,\ \ G = 0.6$$

The values of ω_s and ζ_s were measured in the same manner as in the ground experiment. Fig. 9 shows the results of the experiment, and reveals that the use of the active gyro-stabilizer and the ARFC algorithm suppressed the rolling of the model.

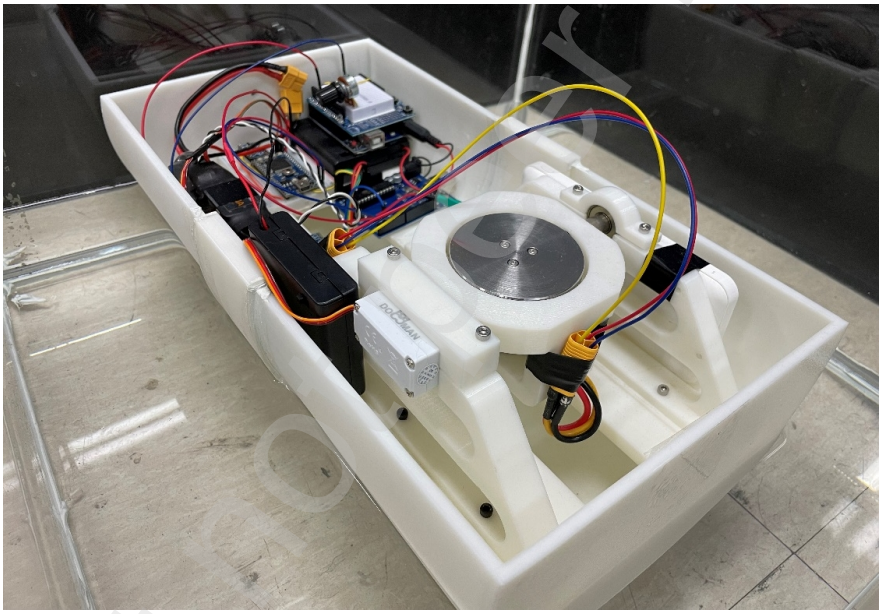

Fig. 8. Experimental setup on the water.

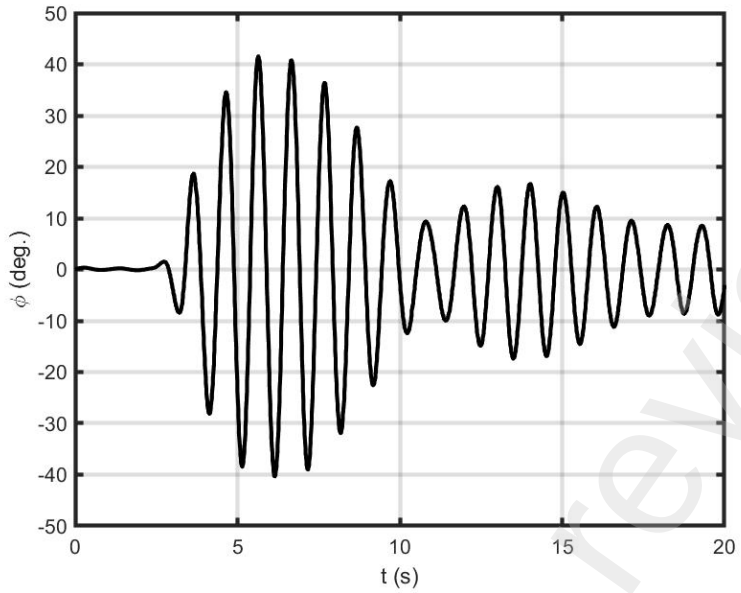

(a) Uncontrolled

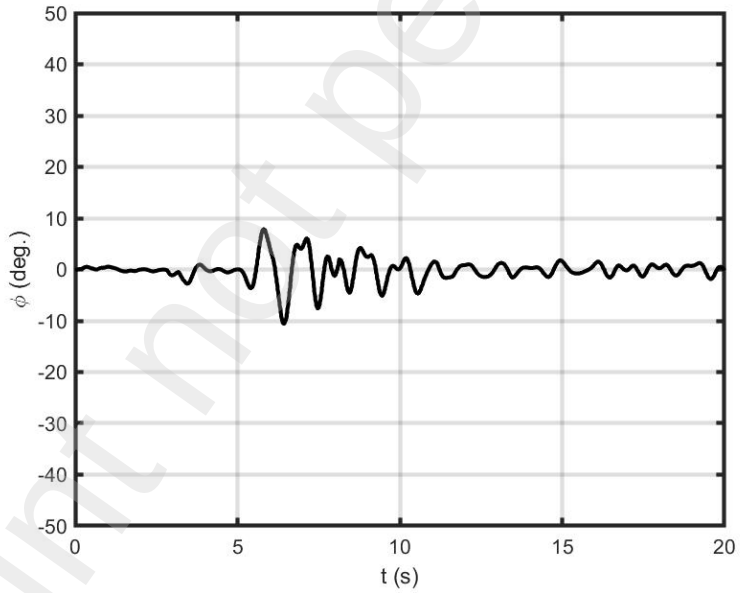

(b) Controlled

Fig. 9. Time response of the roll angle of the ship model on the water.

5. Discussion and Conclusions

In this study, an active gyro-stabilizer was considered as a method to suppress the rolling motion of a ship, and a new control algorithm was developed. First, the equations of motion of the ships with the passive and active gyro-stabilizers were analyzed theoretically, and the validity of the proposed control system was confirmed through numerical calculation. While traditional passive gyro-stabilizers increase stiffness to withstand rolling, the active gyro-stabilizer and the control algorithm proposed in this study can achieve active damping, so can effectively suppress the resonant roll amplitude.

To demonstrate the effectiveness of the active gyro-stabilizer and control algorithm demonstrated through numerical calculation, the experiment was conducted by constructing a ship model, applying an external force, and measuring the roll angle of the model. Experimental results showed that the proposed control algorithm and system are effective even for complex external disturbances.

Because the precession angle is accurately controlled by the servomotor, the control algorithm produces the desired precession angle, and the servomotor controller executes the precise angle tracking using the internal PID controller. The new control algorithm directely uses the angular rate instead of the indirectly estimated angular displacement, so that it eliminates the need to obtain the angular displacement through accelerometer outputs and filtering. The proposed active gyro-stabilizer control algorithm is simple enough that it can be implemented using a microcontroller.

The proposed control algorithm shows the possibility of using a smaller rotor with slower rotational speed and cost-effectiveness. It is proved both theoretically and experimentally that the proposed control algorithm and system can effectively suppress the rolling of the ship

model.

Author contribution

Ki-Seok Song: Methodology, Software, Validation, Formal Analysis, Investigation.

Soo-Min Kim: Validation, Formal Analysis.

Moon K. Kwak: Conceptualization, Supervision, Writing – original draft

Weidong Zhu: Writing – review & editing.

Funding

This research was supported by the MOTIE(Ministry of Trade, Industry, and Energy) in Korea, under the Fostering Global Talents for Innovative Growth Program (P0017307) supervised by the Korea Institute for Advancement of Technology (KIAT)

References

Chalmers, T. W., 1931. The Automatic Stabilisation of Ships. Chapman and Hall, London.

Fanson, J. L., Caughey, T. K., 1990. Positive Position Feedback Control for Large Space Structures. AIAA J. 28 (4), 717-724. https://doi.org/10.2514/3.10451

Harris, C. M., Piersol, A. G., 2002. Harris' shock and vibration handbook, fifth ed. McGraw-Hill, New York, pp. 6.26-6.27.

Jones, R., 1967. The Gyroscopic Vibration Absorber. ASME. J. Ind. 89(4), 706-712.

https://doi.org/10.1115/1.3610140.

Lewis, E. V., 1989. Principles of Naval Architecture : Volume III·Motions in Waves and Controllability. The Society of Naval Architecture and Marine Engineers, Jersey City, NJ.

Manmathakrishnan, P., Pannerselvam, R., 2021. Motion control studies of a barge mounted offshore dynamic wind turbine using gyrostabilizer. Ocean. Eng. 237. https://doi.org/10.1016/j.oceaneng.2021.109578.

Perez, T., 2005. Ship Motion Control : Course Keeping and Roll Stabilisation Using Rudder and Fins. Springer-Verlag London Limited.

Perez, T., Steinmann, P. D., 2009. Analysis of Ship Roll Gyrostabiliser Control. Proceedings of the 8th IFAC International Conference on Maneuvering and Control of Marine Craft. 42(18), 310-315. https://doi.org/10.3182/20090916-3-BR-3001.0007.

Perez, T., Blanke, M., 2012. Ship roll damping control. Annu. Rev. Contr. 36(1), 129-147. https://doi.org/10.1016/j.arcontrol.2012.03.010.

Poh, A. K. -B., Tang, C. H. -H., Kang, H. -S., Lee, K. -Q., Siow, C. -L., Malik, A. M. A., Mailah, M., 2017. Gyroscopic Stabilisation of Rolling Motion in Simplified Marine Hull Model. 2017. IEEE 7th Int. Conf. Underwater System Technology: Theory and Applications. https://doi.org/10.1109/USYS.2017.8309458.

Seakeeper, 2022. Seakeeper Sea Trial Report. https://www.seakeeper.com/performance/ (accessed 22 September 2022).

Schlick, E. O., 1904a. Device for minimizing the oscillatory movements of ships. Patent US 769, 493.

Schlick, E. O., 1904b. The Gyroscopic effect of flywheels on board ship. Trans. Inst. Nav.

Archit. 23(1), 117-134.

Sperry, E. A., 1915. Ship's gyroscope, Patent US 1,150,311.

Townsend, N. C., Murphy, A. J., Shenoi, R. A.,2007. A new active gyrostabilizer system for ride control of marine vehicles. Ocean Eng. 34(11-12), 1607-1617. https://doi.org/10.1016/j.oceaneng.2006.11.004.

Townsend, N. C., Shenoi, R. A., 2014. Control Strategies for Marine Gyrostabilizers. IEEE J. Ocean. Eng. 39, 243-255. https://doi.org/10.1109/JOE.2013.2254591.

Takeuchi, H., Maeda, S., Umemura, K., 2011. Development of the Anti Rolling Gyro 375T(Rolling Stabilizer for Yachts) Using Space Control Technology. Mitsubishi Heavy Ind. Tech. Rev. 48(4), 70-75.

Tustin, A., 1947. A method of analysing the behaviour of linear system in terms of time series. J. Inst. Electr. Eng. – Part IIA: Automatic Regulators and Servo Mechanisms. 94(1), 130-142. https://doi.org/10.1049/ji-2a.1947.0020.

Ünker, F., Çuvalcı, O., 2015. Vibration Control of a Column Using a Gyroscope. Procedia – Soc. Behav. Sci. 195, 2306-2315. https://doi.org/10.1016/j.sbspro.2015.06.182.

Ünker, F., Çuvalcı, O., 2016. Experimental Investigation of a Gyroscopic Vibration Absorber For Vibration Control of a Vertical Cantilever Beam. Proc. of the Fourth Int. Conf. Adv. Civ. Struct. Mech. Eng. 78-82. https://doi.org/10.15224/978-1-63248-093-4-74.

Yang, D. H., Shin, J. H., Lee, H. W., Kim, S. K., Kwak, M. K., 2017. Active vibration control of structure by Active Mass Damper and Multi-Modal Negative Acceleration Feedback control algorithm. J. Sound Vib. 392, 18-30. https://doi.org/10.1016/j.jsv.2016.12.036.